Research Article

Zhenya Zhang, Lucong Han, and Tingxiang Jin*

Analysis and modeling of pitaya slices in a heat pump drying system

https://doi.org/10.1515/phys-2022-0206
received July 06, 2022; accepted October 11, 2022

Abstract: The objective of this article was to investigate the drying kinetics, effective moisture diffusivity, and quality of pitaya in the heat pump drying process. The experiment was conducted at a drying temperature of 50–70°C, slice thickness of 8–10 mm, and a relative humidity of 10–30%. The results showed that the heat pump drying of pitaya was a deceleration process. The drying temperature has the greatest influence on the drying rate. The drying time decreased by 28.57% with the drying temperature increased from 50 to 70°C, while that increased the least by 12% with the slice thickness dropped from 10 to 8 mm. Six drying models were analyzed comparatively based on experimental data, and calculations indicated that the Avhad and Marchetti model could better describe the moisture migration law during the heat pump drying process of pitaya. The optimal drying kinetics model was established to predict the change of moisture content under different drying conditions, and the average error of the model compared with the experimental values was 5.56%. In addition, the effective moisture diffusivity of pitaya ranged from 6.4167×10^{-10} to 9.8156×10^{-10} m^2/s, and the drying temperature had a remarkable influence on the effective moisture diffusivity while the slice thickness had the least. According to the Arrhenius equation, the drying activation energy of pitaya under the experimental conditions was 19.628 kJ/mol. Moreover, the effect of drying temperature on browning degree and surface microstructure was also analyzed. The conclusions of this article provide theoretical support for the analysis of water migration laws and the optimization of the pitaya heat pump drying process.

Keywords: pitaya, heat pump drying, drying kinetics, effective moisture diffusivity, activation energy

1 Introduction

Pitaya is one of the most popular fruits in the world due to its high nutritional value and unique taste [1]. With the expansion of the pitaya planting scale, the yield of pitaya increases year by year. However, pitaya is very perishable due to having a high level of moisture content. The concentrated harvesting of pitaya often leads to fruit decay and deterioration because of poor sales, which will cause a certain waste of resources [2].

Drying technology has been one of the important methods to prolong the storage time of fruits, including hot air drying, vacuum freeze drying, microwave drying, heat pump drying, *etc*. [3]. Appropriate drying methods are an important guarantee for improving fruit storage quality and reducing energy consumption. Hot air drying is widely used to dry fruits and vegetables because of its relatively low cost and simple operation, but hot air drying is easy to cause a decline in the quality of dried fruit and requires a longer drying time [4–6]. Vacuum freeze drying can maximize the retention of nutrients and the quality of dried products. However, vacuum freeze drying has the disadvantages of high cost and energy consumption [7–9]. Microwave drying speed is faster, but it also requires higher costs [10–12]. By contrast, heat pump drying has the advantages of energy saving and no pollution, which can better maintain the flavor and nutrients of dried products. Therefore, it has a great application and development prospect in the fruit drying field [13,14].

In the heat pump drying process, the thin-layer drying kinetics model can analyze the law of moisture migration. Based on this law, the process parameters of heat pump drying can be optimized. In addition, it is also helpful to determine the moisture content of materials under given drying conditions [15]. There exist many studies on thin-layer drying models, but different models

* **Corresponding author: Tingxiang Jin,** School of Energy and Power Engineering, Zhengzhou University of Light Industry, Zhengzhou, 450001, China, e-mail: txjin@126.com
Zhenya Zhang, Lucong Han: School of Energy and Power Engineering, Zhengzhou University of Light Industry, Zhengzhou, 450001, China

have different applicable objects. Zhou *et al.* [16] found that the Page model could accurately predict the drying curve of sludge treated with CaO during the convection drying process. The total cost per unit water loss was the lowest when the drying parameter combination was a CaO addition ratio of 0.02, an air flow rate of 0.6 m/s, and sludge accumulation thickness of 7 mm. Mbegbu *et al.* [17] found that the logarithmic and two-term models could adequately describe the vacuum drying process of scent and lemon basil leaves. The most appropriate temperatures for the drying of scent and lemon basil leaves was found to be 70 and 60°C, respectively.

To the best of the author's knowledge, there are few research on drying kinetics in the pitaya heat pump process in the existing literature. Extensive researches were conducted on the drying kinetics and drying models of similar fruits and vegetables. Tunckal and Doymaz [18] found that the Midilli–Kucuk model could better describe the banana heat pump drying process. The range of effective moisture diffusion coefficient was 1.12×10^{-10} to 1.64×10^{-10} m^2/s and the activation energy was 51.45 kJ/mol. Peter *et al.* [19] found that the Midilli–Kucuk model was the most superior thin-layer drying model in predicting the drying kinetics of chanterelle mushrooms. Artificial neural network architecture was the best architecture in predicting the drying process of chanterelle mushrooms, and the Support Vector Machine model could be used for online monitoring and control of the heat pump drying process of chicken oil fungus. Gasa *et al.* [20] found that compared with natural ventilation and solar venturi dryer, the drying rate of hot air drying was faster. Under natural ventilation conditions, increasing the air flow rate could effectively improve the drying efficiency of solar venturi dryers for sweet potato chips. The Midilli–Kucuk model was the most accurate to describe the hot air drying process. Xie *et al.* [21] studied the effects of different drying methods on the dynamic model of peanut drying. They found that radio frequency combined hot air drying required the shortest drying time for peanuts drying. The Weibull model was optimum to describe the moisture ratio (MR) of peanuts during the drying process. Kong *et al.* [22] studied the drying of radishes by an indirect solar drying system. They found that the Midilli–Kucuk model was considered suitable to describe the drying process of radish slices. The total color difference between radishes with natural drying and solar drying was the highest. The drying method using solar drying equipment was superior to natural drying in cloudy weather. Dhurve *et al.* [23] studied the convective disk drying of watermelon seeds and found that the Midilli–Kucuk model fitted the experimental drying best. The specific energy consumption decreased with the increase in temperature with a moderate activation energy of 27.66 kJ/mol, and 60°C was the most suitable temperature for watermelon seed drying. Biswas *et al.* [24] studied the effects of different osmotic pretreatment on hot air drying of pineapple slices. They found that the logarithmic model could describe the drying process precisely. The average error percentage of the Page model fitting was low (2.188–7.479%). The ideal combination was at a drying temperature of 55°C, 30% relative humidity, and 1% trehalose solution permeation pretreatment. Granella *et al.* [25] studied the effect of pretreatment on banana slices in the convection process. The Page model was the most accurate in their conclusion. Drying pretreatment could promote convective drying, reducing drying time by up to 31%, and saving energy by 19%. The banana slices pretreated with ethanol and ultrasonic were of the best quality.

Based on the current research on pitaya drying, there is little information about the drying kinetics and the drying models of the pitaya heat pump drying process. In this article, the drying kinetics of pitaya during the heat pump drying process was studied under different drying temperatures, slice thickness, and relative humidity. The variation model of MR was analyzed and the accurate MR model of pitaya heat pump drying was obtained and verified. In addition, the effective water diffusion coefficient and activation energy of pitaya was calculated using the Arrhenius equation. Moreover, the effects of different drying conditions on browning degree and surface microstructure were compared. The conclusions aim to provide technical support for reducing heat pump drying energy consumption, improving product quality, and optimizing process parameters of heat pump drying.

2 Materials and methods

2.1 Experimental process

The pitaya drying process is shown in Figure 1. At first, a white heart pitaya with moderate size, no pests, and no mechanical damage bought from a local market (Zhengzhou, China) was selected before the experiment. After being peeled and cleaned by a slicer (Hengna Catering Equipment Co., Ltd, Guangzhou, China), pitaya was sliced into 8,

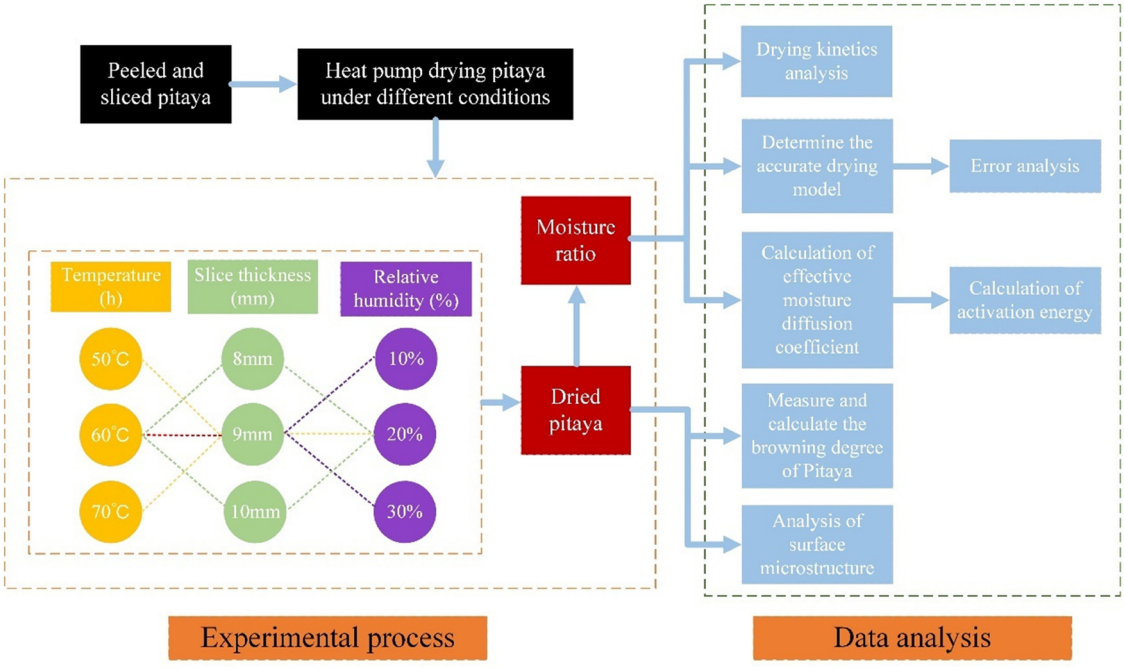

Figure 1: Experimental flow chart.

9, and 10 mm-thick slices with a side length of 50 mm. The samples are shown in Figure 2.

Second, the heat pump dryer was operated for at least 30 min until reached a stable state before the experiment. When the system reached the stable temperature, the fresh pitaya slices without any pretreatment were put into the heat pump dryer (Chuanglu Refrigeration Technology Co., Ltd, Guangdong, China) for drying, precision electronic balance (De ante Sensing Technology Co., Ltd, Tianjin, China) was used to record the weight every hour until the weight remain unchanged. At this point, the pitaya drying process was considered complete. Then, pitaya samples treated at different drying temperatures were cut into squares with a side length of 1 mm, pasted on the copper plate, and then sprayed with gold. After the device is vacuumized, the microstructure of the sample is observed and photographed by scanning electron microscope (JSM-6490LV; Credit Rating Agency Ltd, Japan).

Figure 2: Fresh pitaya sample.

2.2 Drying kinetics model

The dry base moisture content (W_d) of the pitaya is calculated according to the following Eq. (1) [26]:

$$W_d = \frac{m_w - m_d}{m_d}, \tag{1}$$

where, m_w and m_d represent the quality of pitaya at time T and the absolute dry quality of pitaya, respectively.

The drying rate (D_R) is calculated according to the following equation [27]:

$$D_R = \frac{M_{t+dt} - M_t}{d_t}, \tag{2}$$

where, M_{t+dt} and M_t represent the moisture content of the sample at time $t + dt$ and t, respectively.

The MR is calculated as follows [28]:

$$MR = \frac{M_t - M_e}{M_0 - M_e}, \tag{3}$$

where, M_e and M_0 represent the equilibrium dry base moisture content and initial dry base moisture content of the sample, respectively. M_e is negligible as M_t and M_0. Therefore, Eq. (3) becomes

$$MR = \frac{M_t}{M_0}. \tag{4}$$

The drying process of pitaya belongs to thin-layer drying. In order to obtain a drying model that can accurately describe the law of water migration during the heat pump drying process of pitaya, the MR obtained from the experiment was fitted and analyzed with six commonly used thin-layer drying models as shown in Table 1.

The model parameters were determined by nonlinear analysis based on Levenberg–Marquardt algorithm. The fitting degree was evaluated by correction coefficient (R^2), residual square sum (RSS) of predicted moisture value, and reducing chi-square (χ^2). These parameters are defined using Eqs. (5)–(7) [35].

$$R^2 = 1 - \frac{\sum_{i=1}^{n}(\mathrm{MR}_{\mathrm{cal},i} - \mathrm{MR}_{\mathrm{exp},i})^2}{\sum_{i=1}^{n}(\overline{\mathrm{MR}_{\mathrm{cal},i}} - \mathrm{MR}_{\mathrm{exp},i})^2}, \tag{5}$$

$$\mathrm{RSS} = \sum_{i=1}^{n}(\mathrm{MR}_{\mathrm{cal},i} - \mathrm{MR}_{\mathrm{exp},i})^2, \tag{6}$$

$$\chi^2 = \frac{\sum_{i=1}^{n}(\mathrm{MR}_{\mathrm{cal},i} - \mathrm{MR}_{\mathrm{exp},i})^2}{n - m}, \tag{7}$$

where $\mathrm{MR}_{\mathrm{exp},i}$ and $\mathrm{MR}_{\mathrm{cal},i}$ represent the test value and calculated value of water ratio, respectively; n and m represent the number of test values and calculated values, respectively.

Table 1: Thin layer drying model

Number	Models	Expressions
1	Lewis (Newton) [29]	$MR = \exp(-kt)$
2	Avhad and Marchetti [30]	$MR = a\exp(-kt^n)$
3	Henderson and Pabis [31]	$MR = a\exp(-kt)$
4	Wang and Singh [32]	$MR = 1 + at + bt^2$
5	Two-term exponential [33]	$MR = A_0\exp(-k_0t) + (1 - A_0)\exp(-k_0A_0t)$
6	Logarithmic [34]	$MR = a\exp(-kt) + c$

2.3 Determination of effective moisture diffusivity

According to Fick's law and Arrhenius equation, the effective moisture diffusion coefficient D_{eff} is obtained as shown in the following equation [36]:

$$\mathrm{MR} = \frac{8}{\pi^2}\exp\left(-\frac{\pi^2 D_{\mathrm{eff}}}{L^2}t\right). \tag{8}$$

Eq. (8) is converted into logarithmic form as Eq. (9) as follows:

$$\ln \mathrm{MR} = \ln\frac{8}{\pi^2} - \frac{\pi^2 D_{\mathrm{eff}}}{L^2}t. \tag{9}$$

The slope k_1 is calculated from the function of ln MRon T, thus the D_{eff} is obtained, where L and t represent the thickness (m) and the drying time (s) of dry material, respectively.

$$k_1 = -\frac{\pi^2 D_{\mathrm{eff}}}{L^2}. \tag{10}$$

2.4 Determination of activation energy

Combined with effective moisture diffusion coefficient D_{eff} and drying temperature T, according to Arrhenius equation. the activation energy E_a is calculated as follows [37]:

$$D_{\mathrm{eff}} = D_0\exp\left[-\frac{E_a}{R(T + 273.15)}\right], \tag{11}$$

where D_0 represents the moisture diffusion constant (m^2/s; R represents the gas constant, and its value is 8.314 J/(mol K); T is the temperature (°C). Eq. (12) can be obtained by transforming Eq. (11) into the logarithmic form:

$$\ln D_{\mathrm{eff}} = \ln D_0 - \frac{E_a}{R}\cdot\frac{1}{T + 273.15}. \tag{12}$$

$\ln D_{\mathrm{eff}}$ has a linear relationship with $1/(T + 273.15)$, thus E_a is obtained as follows:

$$k_2 = -\frac{E_a}{R}. \tag{13}$$

2.5 Determination of browning degree

The browning degree of dried pitaya under different conditions was studied in detail. First, the spectrophotometric colorimeter (3NH Technology Co., Ltd, Shenzhen, China) was calibrated against the calibration board. Second, the

device was set to specular component include measurement mode, D65 light source, and CIE Lab color space. Third, the brightness value L_0^*, red–green value a_0^*, and yellow–blue value b_0^* of pitaya fresh fruit with the color difference meter were gauged. Finally, the brightness value L^*, red–green value a^*, and yellow–blue value b^* of the pitaya sample after heat pump drying were measured [38]. The total color difference ΔE value can be obtained by Eq. (14) [39], and the browning degree browning index (BI) value can be obtained by Eqs. (15) and (16) [40]. In order to improve the accuracy of data, the samples were homogenized before the test, and the average BI was taken after five measurements for each group of samples.

$$\Delta E = \sqrt{(L^* - L_0^*)^2 + (a^* - a_0^*)^2 + (b^* - b_0^*)^2}, \quad (14)$$

$$x = \frac{a^* + 1.75L^*}{5.645L^* + a - 3.012b^*}, \quad (15)$$

$$\mathrm{BI} = \frac{x - 0.31}{0.172} \times 100, \quad (16)$$

where L_0^*, a_0^*, and b_0^* are color parameters of fresh pitaya; L, a, and b are the color parameters of dried pitaya samples.

3 Results and discussion

3.1 Drying kinetics

The MR and drying rate of the pitaya heat pump drying at different drying temperatures are shown in Figure 3. As shown in Figure 3(a), when the slice thickness and relative humidity remained unchanged, the drying time required to reach the drying standard was found to be 20, 24, and 28 h at 50, 60, and 70°C, respectively, and the drying rate decreased 28.57% with the drying temperature rising from 50 to 70°C. Similar drying behaviors were reported for the hot air drying of black ginger [41]. High temperature caused an increase in the temperature gradient between pitaya and surrounding air in the drying chamber, as well as an increase in the diffusion rate of water molecules and the rate of surface evaporation, which increases the drying rate. In addition, it can be seen from Figure 3(b) that the drying process was a deceleration process, the reason was that the bound water content in slices decreased with the drying process, resulting in a decrease in the water vapor pressure gradient.

The MR and drying rate of the pitaya heat pump drying at different slice thicknesses are shown in Figure 4. Under the condition of constant drying temperature and relative humidity, the drying time for 8, 9, and10 mm thickness samples were 22, 24, and 25 h, respectively. The drying time at higher slice thickness (10 mm) decreased by 12% as that of 8 mm. A similar trend was reported for the hot drying of mango by Aman et al. [42]. The products with thinner slices dried faster because of the reduced water migration distance and the increased relative surfaced area exposed for a given volume of dried product.

The MR and drying rate of the pitaya heat pump drying at different relative humidity are shown in Figure 5. It was found that the drying rate increased with the

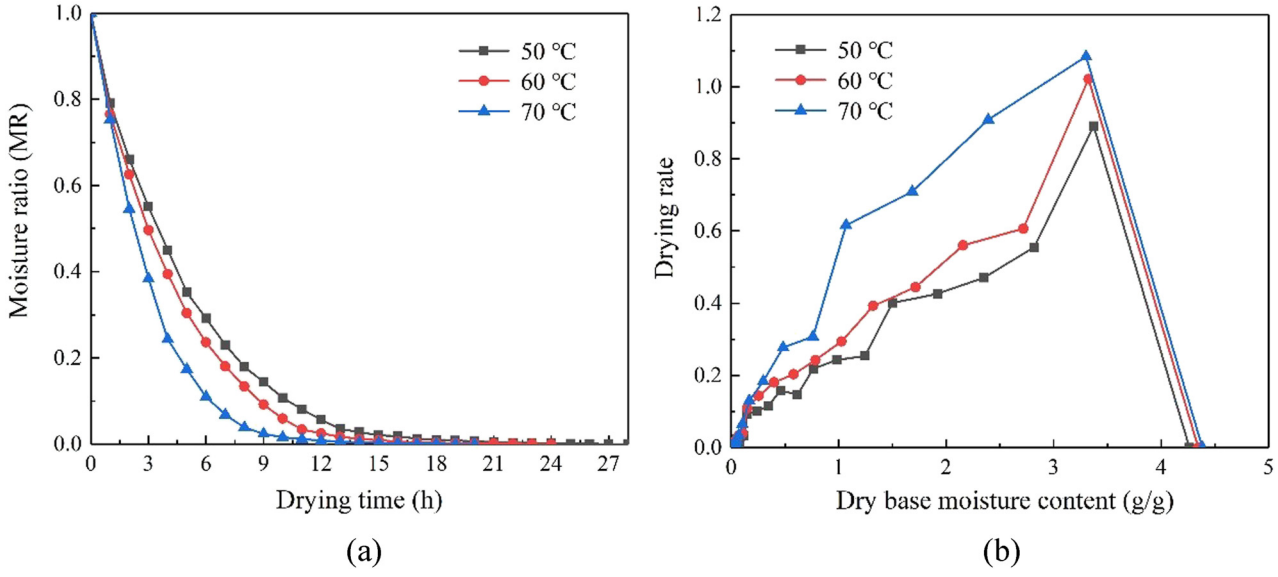

Figure 3: MR (a) and drying rate (b) of pitaya slices at different heat pump drying temperatures.

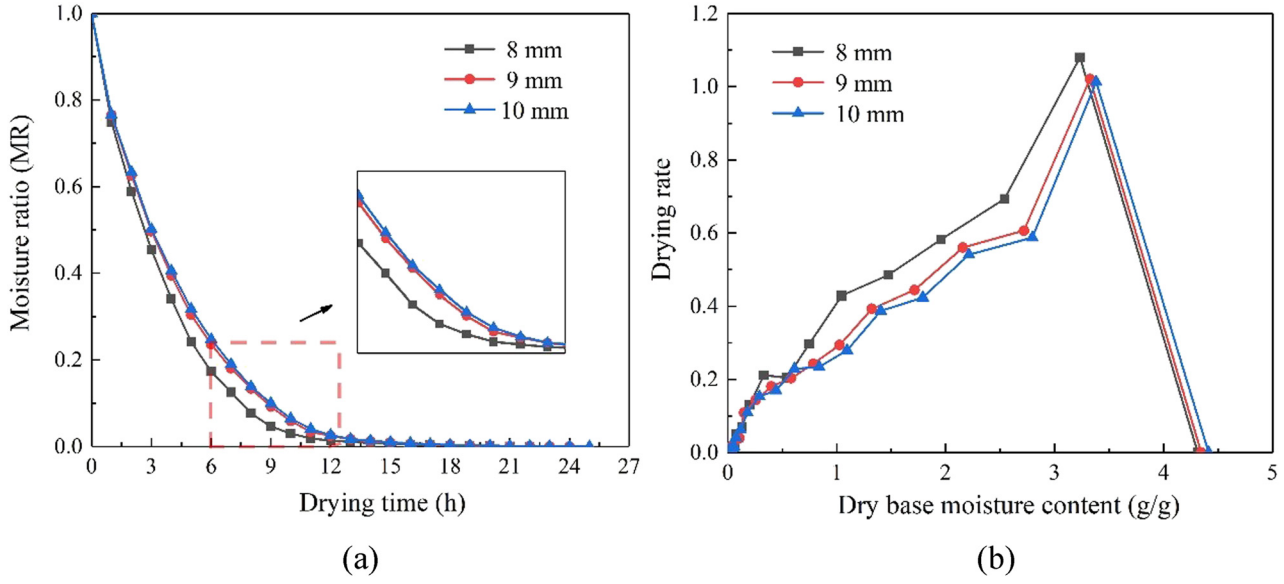

Figure 4: MR (a) and drying rate (b) of pitaya slices with different slice thicknesses.

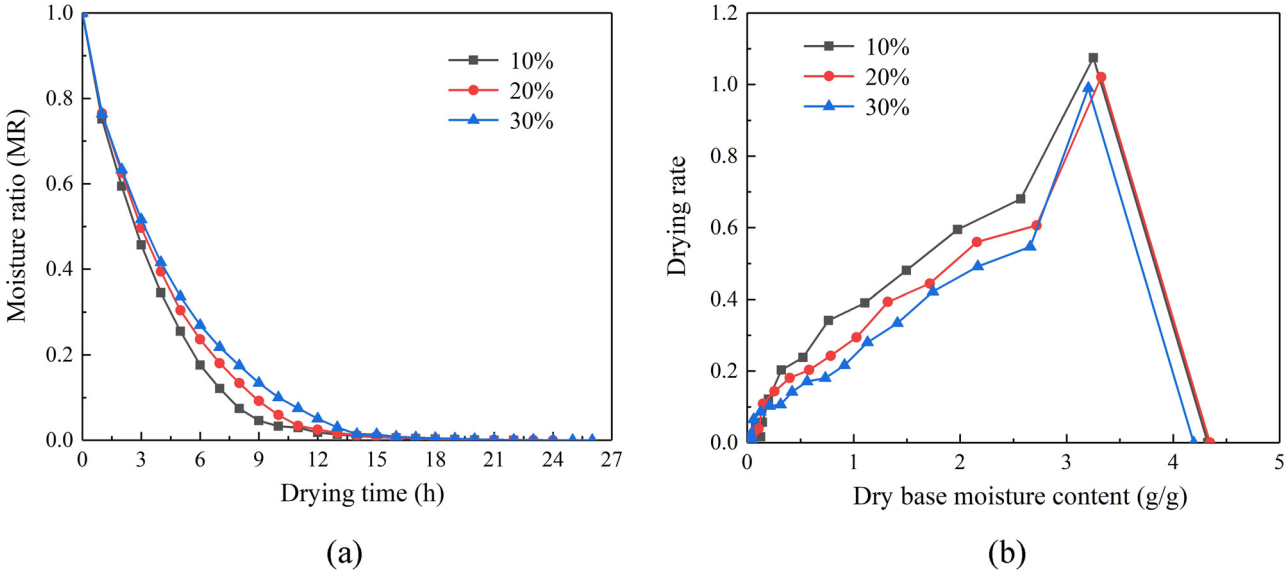

Figure 5: MR (a) and drying rate (b) of pitaya slices under different relative humidity.

decrease in relative humidity when the drying temperature and slice thickness were constant. The drying time increased from 22 to 26 h with the relative humidity increased from 10 to 30%, rising by 15.38%. According to Fick's law and its boundary conditions, the decrease of relative humidity leads to the increase of water vapor pressure difference between material and environment, which results in the increase of the driving force, thus shortening the drying time and improving drying efficiency, this conclusion is consistent with the study on apple conducted by Ramirez *et al.* [43]

3.2 Model calculating and validation

3.2.1 Model calculating and selection of the best model

By calculating the experimental data with six thin-layer drying models, the model parameter values and evaluation index results of pitaya slices under different drying conditions were obtained as shown in Tables 2–7.

The correction coefficient (R^2) reflects the proportion that all variations of dependent variables can be explained by independent variables through regression relationships.

Table 2: Statistical analysis of the Lewis (Newton) model

Experimental conditions			Model parameters	Evaluation index		
Drying temperature (°C)	Slice thickness (mm)	Relative humidity (%)	k	R^2	RSS	χ^2
50	9	20	0.2138	0.9962	0.005	1.86×10^{-4}
60			0.248	0.9946	0.006	2.59×10^{-4}
70			0.3394	0.9917	0.0069	3.63×10^{-4}
60	8	20	0.2865	0.9941	0.0057	2.72×10^{-4}
	9		0.248	0.9946	0.006	2.59×10^{-4}
	10		0.242	0.9943	0.0065	2.72×10^{-4}
60	9	10	0.2829	0.9939	0.0059	2.82×10^{-4}
		20	0.248	0.9946	0.006	2.59×10^{-4}
		30	0.2267	0.9957	0.005	2.02×10^{-4}

Table 3: Statistical analysis of the Henderson and Pabis model

Experimental conditions			Model parameters		Evaluation index		
Drying temperature (°C)	Slice thickness (mm)	Relative humidity (%)	a	k	R^2	RSS	χ^2
50	9	20	1.0183	0.2175	0.9964	0.0048	1.83×10^{-4}
60			1.023	0.2533	0.9949	0.0056	2.56×10^{-4}
70			1.1232	0.3775	0.9977	0.0019	1.07×10^{-4}
60	8	20	1.0471	0.2989	0.9952	0.0046	2.32×10^{-4}
	9		1.023	0.2533	0.9949	0.0056	2.56×10^{-4}
	10		1.0195	0.2464	0.9945	0.0063	2.73×10^{-4}
60	9	10	1.0473	0.2953	0.995	0.0048	2.41×10^{-4}
		20	1.023	0.2533	0.9949	0.0056	2.56×10^{-4}
		30	0.9849	0.2235	0.9959	0.0049	2.03×10^{-4}

Table 4: Statistical analysis of the Avhad and Marchetti model

Experimental conditions			Model parameters			Evaluation index		
Drying temperature (°C)	Slice thickness (mm)	Relative humidity (%)	a	k	n	R^2	RSS (10^{-4})	χ^2 (10^{-5})
50	9	20	0.8881	0.1212	1.2461	0.9996	4.67	1.87
60			0.8627	0.1273	1.3071	0.9994	6.27	2.98
70			0.9551	0.2373	1.2385	0.9997	2.49	1.46
60	8	20	0.8657	0.1487	1.3336	0.9997	2.74	1.44
	9		0.8627	0.1273	1.3071	0.9994	6.27	2.98
	10		0.8567	0.1196	1.3197	0.9994	7.07	3.21
60	9	10	0.866	0.1456	1.3374	0.9996	4.08	2.14
		20	0.8627	0.1273	1.3071	0.9994	6.27	2.98
		30	0.8601	0.1275	1.2369	0.999	12	5.16

The RSS reflects the square sum of the difference between the actual value and the predicted value. The reduced chi-square (χ^2) is used to test the correlation of data. When the R^2 was the highest, RSS and χ^2 were the lowest, the deviation degree and difference degree between the experimental value and the calculated value were the smallest, and the model could best describe the drying process. According to the calculation of the results in Tables 2–7 above, it was found that the R^2 value of the Avhad and Marchetti model was the largest (0.999–0.9997), while the value of RSS (2.49×10^{-4}~$1.2. \times 10^{-3}$) and χ^2 (1.44×10^{-5} ~5.16×10^{-5}) were the smallest. Therefore, the Avhad and Marchetti model was the most accurate model to describe the heat pump drying process of pitaya.

Table 5: Statistical analysis of the Wang and Singh model

Experimental conditions			Model parameters		Evaluation index		
Drying temperature (°C)	Slice thickness (mm)	Relative humidity (%)	a	b	R^2	RSS	χ^2
50	9	20	−0.1144	0.003	0.8261	0.2298	0.0088
60			−0.1333	0.0041	0.8297	0.1889	0.0086
70			−0.1667	0.0062	0.7165	0.2366	0.0131
60	8	20	−0.1482	0.0049	0.7842	0.2077	0.0104
	9		−0.1333	0.0041	0.8297	0.1889	0.0086
	10		−0.1287	0.0038	0.8207	0.206	0.009
60	9	10	−0.1475	0.005	0.7904	0.2037	0.0102
		20	−0.1333	0.0041	0.8297	0.1889	0.0086
		30	−0.1221	0.0034	0.8237	0.2077	0.0087

Table 6: Statistical analysis of the two-term exponential model

Experimental conditions			Model parameters		Evaluation index		
Drying temperature (°C)	Slice thickness (mm)	Relative humidity (%)	A_0	k_0	R^2	RSS	χ^2
50	9	20	1.5005	0.2523	0.998	0.0026	1.02×10^{-4}
60			1.5182	0.2952	0.997	0.0034	1.53×10^{-4}
70			1.6997	0.4462	0.9995	3.97E-4	2.21×10^{-5}
60	8	20	1.5725	0.351	0.9977	0.0023	1.13×10^{-4}
	9		1.5182	0.2952	0.997	0.0034	1.53×10^{-4}
	10		1.5145	0.2874	0.9966	0.0039	1.7×10^{-4}
60	9	10	1.5759	0.3474	0.9975	0.0024	1.2×10^{-4}
		20	1.5182	0.2952	0.997	0.0034	1.53×10^{-4}
		30	1.3765	0.2516	0.9963	0.0044	1.84×10^{-4}

Table 7: Statistical analysis of the logarithmic model

Experimental conditions			Model parameters			Evaluation index		
Drying temperature (°C)	Slice thickness (mm)	Relative humidity (%)	a	k	n	R^2	RSS	χ^2 (10^{-4})
50	9	20	1.0149	0.2066	−0.0128	0.9976	0.0031	1.25
60			1.0179	0.238	−0.015	0.9968	0.0036	1.7
70			1.1181	0.3684	−0.0058	0.9981	0.0016	0.947
60	8	20	1.0416	0.2854	−0.0113	0.9964	0.0035	1.84
	9		1.0179	0.238	−0.015	0.9968	0.0036	1.7
	10		1.0148	0.2317	−0.0153	0.9964	0.0041	1.88
60	9	10	1.0422	0.2827	−0.0106	0.9961	0.0038	2.02
		20	1.0179	0.238	−0.015	0.9968	0.0036	1.7
		30	0.9806	0.2086	−0.0167	0.9979	0.0025	1.08

3.2.2 The determination of parameters in the model

The parameters a, k, and n in the Avhad and Marchetti model are related to the test conditions (drying temperature [T], slice thickness [L], and relative humidity [RH]). Different test conditions correspond to different parameter values. The parameters a, k, and n can be defined as the linear function of these variables, *i.e.*,

$$a = \alpha_A + \beta_A T + \gamma_A L + \chi_A \mathrm{RH}, \tag{17}$$

$$k = \alpha_B + \beta_B T + \gamma_B L + \chi_B \mathrm{RH}, \quad (18)$$

$$n = \alpha_C + \beta_C T + \gamma_C L + \chi_C \mathrm{RH}, \quad (19)$$

where α, β, γ and χ represent undetermined coefficients.

The calculation results of Avhad and Marchetti model were used for linear fitting of parameters a, k, and n, and the values of undetermined coefficients α, β, γ, and χ were obtained and substituted into the above formula, hence we obtain

$$a = 0.7209 + 0.0035T - 0.0045L - 0.000295\mathrm{RH}, \quad (20)$$

$$k = -0.0568 + 0.0058T - 0.0145L - 0.0009\mathrm{RH}, \quad (21)$$

$$n = 1.4785 - 0.00038T - 0.00069L - 0.005\mathrm{RH}. \quad (22)$$

Substitute the model parameters a, k, and n obtained by fitting into the Avhad and Marchetti model, and the mathematical model of pitaya heat pump drying was obtained as follows:

$$MR = (0.7209 + 0.0035T - 0.0045L - 0.000295RH) \times \exp((-0.0568 + 0.0058T - 0.0145L - 0.0009RH)t^{(1.4785-0.00038T-0.00069L-0.005RH)}). \quad (23)$$

3.3 Model validation

In order to test the accuracy of the mathematical model, a verification experiment was carried out under the drying conditions of 60°C drying temperature, 9 mm slice thickness, and 20% relative humidity. The comparison results between experimental values and calculated values are shown in Figure 6. The variation trend of the experimental value was consistent with that of the calculated value. The maximize and average error was 10.36% and 5.56%, respectively, compared with the experimental value, indicating that the Avhad and Marchetti model could accurately predict the moisture change in the pitaya heat pump drying process.

3.4 Effective moisture diffusivity

The effective moisture diffusion coefficient represents the diffusion of water in the drying process of the material and reflects the dehydration ability of materials under certain conditions [44]. The effective moisture diffusion coefficient of pitaya slices under different heat pump drying conditions was calculated through Eqs. (8)–(10). It can be seen from Table 8 that the effective moisture diffusion coefficient increased from 6.4167×10^{-10} to 9.8156×10^{-10} m^2/s when the drying temperature increased from 50 to 70°C, this conclusion is consistent with the study on lentil crop conducted by Heydari *et al.* [45]. The permeability of the cell wall increases and the internal water escapes easily with high temperatures, accelerating the diffusion and migration rate of water molecules, thus the effective water diffusion coefficient was increased. The effective moisture diffusion coefficient decreased from 8.0193×10^{-10} to 8.2666×10^{-10} m^2/s with the slice thickness increased from 8 to 10 mm. With the increase of the slice thickness, the evaporation distance of the internal bound water increases, leading to the increase of migration resistance, resulting in the decrease of the effective moisture diffusion coefficient. When the drying temperature

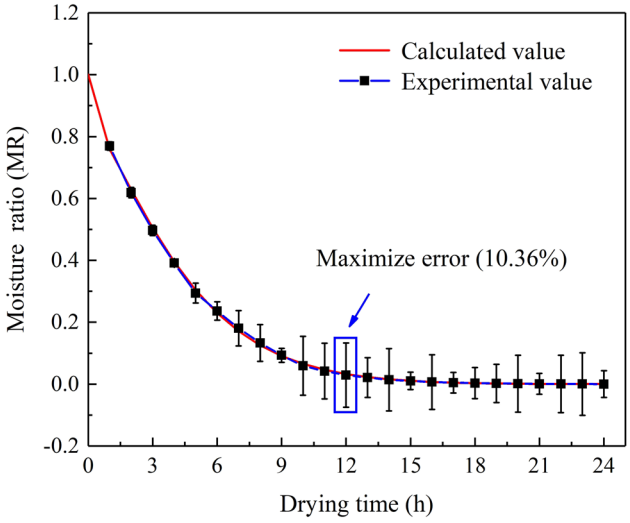

Figure 6: Comparison between experimental values and calculated values.

Table 8: Effective moisture diffusivity of pitaya under different heat pump drying conditions

Experimental conditions			Effective moisture diffusivity (m^2/s)
Drying temperature (°C)	Slice thickness (mm)	Relative humidity (%)	
50	9	20	6.4167×10^{-10}
60			8.2406×10^{-10}
70			9.8156×10^{-10}
60	8	20	8.2666×10^{-10}
	9		8.2406×10^{-10}
	10		8.0193×10^{-10}
60	9	10	8.3361×10^{-10}
		20	8.2406×10^{-10}
		30	7.8243×10^{-10}

and slice thickness remained unchanged, the relative humidity increased from 10 to 30%, and the effective moisture diffusivity decreased from 8.3361×10^{-10} to 7.8243×10^{-10} m^2/s. The higher water vapor pressure gradient on the surface of the material was created after the reduction in relative humidity, which made the water on the surface of the material evaporated faster, thus improving the effective moisture diffusivity.

3.5 Activation energy

Activation energy refers to the energy required for the material to remove the amount of water per unit of material in the drying process. Large activation energy means that more energy is required for drying, and the material is more difficult to dry. Combined with the effective moisture diffusion coefficient D_{eff} and drying temperature T, according to the Arrhenius equation, $\ln D_{\text{eff}}$ has a linear relationship with $1/(T + 273.15)$ and the slope is $-\frac{E_0}{R}$.

As can be seen from Figure 7, when the slice thickness is 9 mm and the relative humidity is 20%, the slope corresponds to the logarithm of the effective moisture diffusion coefficient of the pitaya slice is −2360.82. By substituting into Eq. (13), the drying activation energy of the pitaya slice is 19.628 kJ/mol, indicating that under the drying conditions of slice thickness of 9 mm and relative humidity of 20%. The minimum energy required to remove 1 mol of water from pitaya is 19.628 kJ/mol.

3.6 Effect of a single factor on the browning degree of dried pitaya

It can be seen from Figure 8 that the browning degree of dried pitaya increases with the increase in drying temperature and relative humidity and the decrease in slice thickness. The drying temperature had the most obvious effect on it, while the slice thickness had the least. The browning degree increased from 17.86 to 35.35 with the drying temperature rising from 50 to 70°C at a thickness of 9 mm and relative humidity of 20%, which significantly increased by 97.93%. Figure 9 shows the dried pitaya at different drying temperatures, and the obvious color difference between them can be easily observed. The conclusion agreed with the study of Pan *et al.* on areca nut [46]. In contrast, the browning decreased from 26.99 to 18.72 with the slice thickness increased from 8 to 10 mm at the temperature of 60°C and relative humidity of 20%. The browning degree was reduced by 30.64%. The main cause of the browning degree of dried products is the Maillard reaction, which is a non-enzymatic browning reaction widely used in the food industry. The slice temperature of pitaya obviously increased with the higher drying temperature and thinner slice thickness, which promoted the Maillard reaction and resulted in a high browning degree of pitaya slices. In addition, the moisture content of pitaya decreases slowly when the relative humidity is high, which makes the moisture content of pitaya slices stay in the range where the Maillard reaction is prone to occur for a long time and finally leads to the increase of browning

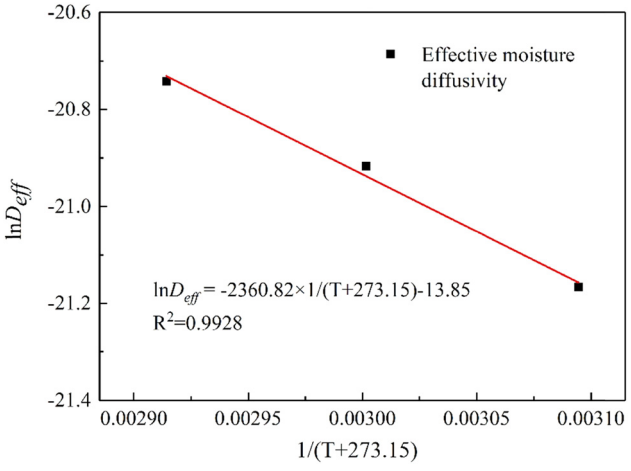

Figure 7: Water diffusion coefficient of pitaya slices at different drying temperatures.

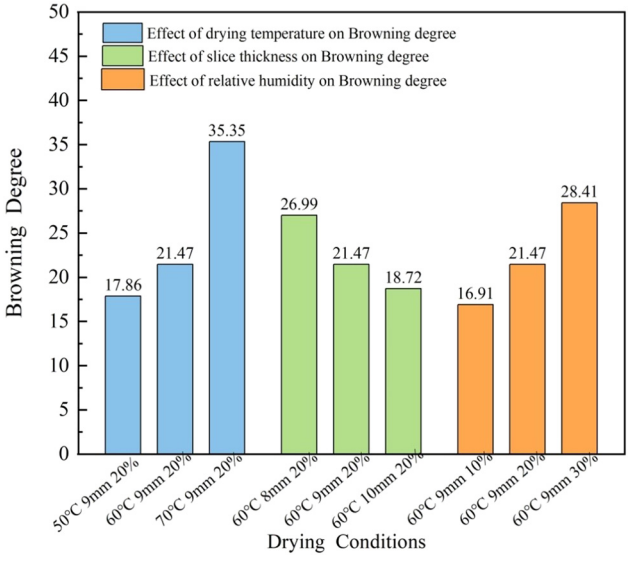

Figure 8: Effect of drying conditions on browning degree of dried pitaya.

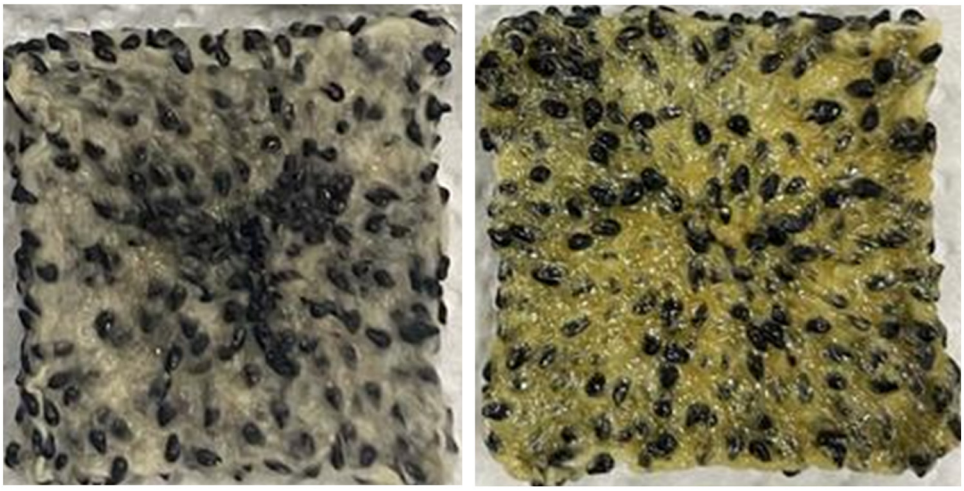

(a) (b)

Figure 9: Dried pitaya samples at different drying temperatures: (a) 50°C, 9 mm, 20% and (b) 70°C, 9 mm, 20%.

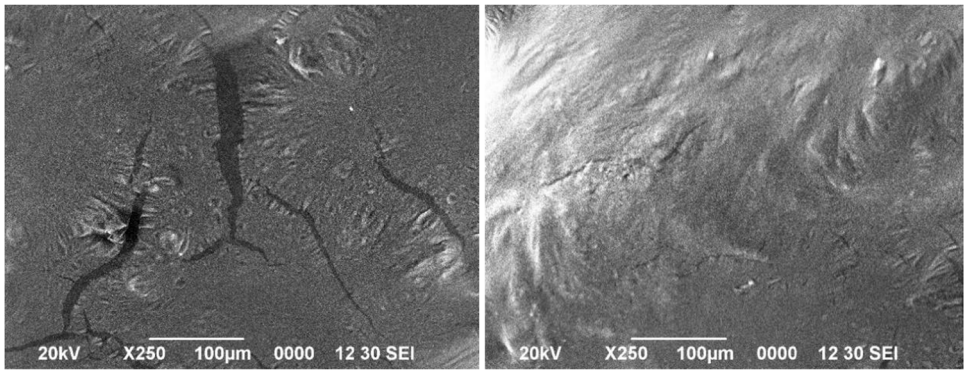

(a) (b)

Figure 10: Surface microstructure of dried pitaya at (a) 70°C, 9 mm, 20% and (b) 50°C, 9 mm, 20%.

degree [47]. Therefore, lower drying temperature, relative humidity, and larger slice thickness should be used to make the water content of pitaya leave the Maillard reaction zone as soon as possible, so as to obtain the dried products with less browning degree.

3.7 Effect of drying temperature on the surface microstructure of dried pitaya

According to the above analysis, when the slice thickness and relative humidity remain unchanged, the difference in browning degree between the two samples dried at 50 and 70°C was the largest. Two samples with a slice thickness of 9 mm, relative humidity of 20%, and drying temperature of 50 and 70°C were selected for surface microstructure analysis as shown in Figure 10. It can be seen that there are great differences in the surface microstructure of pitaya slices dried by different drying temperatures. When the drying temperature is 70°C, the surface of the pitaya slices is uneven and cracked, but it is smoother and the cracks are few at 50°C. The heat and mass transfer process of pitaya is obviously accelerated due to high temperature, the increase in temperature gradient enhances the water evaporation rate on the surface of the pitaya, resulting in the contraction of pitaya slices [48,49].

4 Conclusion

The main research content of this article is to analyze the drying dynamics of pitaya in the process of heat pump drying by using the thin-layer model. The conclusions are as follows:

1) The heat pump drying of pitaya was a deceleration process, the drying temperature had the most obvious effect on the drying rate, while the slice thickness had the least. The drying time decreased by 28.57% with the drying temperature increased from 50 to 70°C, while that increased the least by 12% with the slice thickness dropped from 10 to 8 mm.
2) Based on the comparative analysis of six thin-layer drying models, it was found that the Avhad and Marchetti model was the most suitable to describe the pitaya heat pump drying process. According to the experimental conditions of this article, the variation law of MR under different drying conditions was determined by the mathematical model, and the average error of the model was within 5.56% compared with the experimental value.
3) Under the test conditions in this article, the effective moisture diffusivity ranged from 6.4167×10^{-10} to 9.8156×10^{-10} m^2/s. The effective moisture diffusion coefficient was obviously affected by drying temperature while the slice thickness had the least influence on it. Moreover, the drying activation energy of pitaya was 19.628 kJ/mol.
4) The browning degree of dried pitaya was positively correlated with the increase in drying temperature and relative humidity and negatively correlated with the increase in slice thickness. The browning degree significantly increased by 97.93% with the drying temperature rising from 50 to 70°C. Higher temperatures will lead to the fact that dried pitaya has more wrinkles and cracks on its surface.

The research results provide a theoretical reference for the energy consumption analysis and quality improvement for pitaya heat pump drying. Moreover, proper pretreatment before drying can also improve the drying rate and the quality of the dried pitaya. In the following research work, the technical scheme of reducing the heat pump drying consumption and improving the quality of pitaya will be further analyzed combined with the pretreatment technology.

Funding information: This work was supported by the Doctoral Scientific Research Foundation of Zhengzhou University of Light Industry (Grant No. 2020BSJJ082), the Postgraduate education innovation training base project of Henan Province (Grant No. YJS2021JD05), and the Henan Provincial Department of Science and Technology Research Project (Grant No. 222102320075).

Author contributions: All authors have accepted responsibility for the entire content of this manuscript and approved its submission.

Conflict of interest: The authors state no conflict of interest.

References

[1] Jiang H, Zhang W, Li X, Shu C, Jiang W, Cao J. Nutrition, phytochemical profile, bioactivities and applications in food industry of pitaya (*Hylocereus* spp.) peels: A comprehensive review. Trends Food Sci Tech. 2021;116:199–217.
[2] Li Z, Li B, Li M, Fu X, Zhao X, Min D, et al. Hot air pretreatment alleviates browning of fresh-cut pitaya fruit by regulating phenylpropanoid pathway and ascorbate-glutathione cycle. Postharvest Biol Tec. 2022;190:111954.
[3] Wen X, Li W, Li W, Chen W, Zhang Z, Wu D, et al. Quality characteristics and non-volatile taste formation mechanism of Lentinula edodes during hot air drying. Food Chem. 2022;393(1):133378.
[4] Elik A. Hot air-assisted radio frequency drying of black carrot pomace: Kinetics and product quality. Innov Food Sci Emerg. 2021;73:102800.
[5] Onwude D, Hashim N, Abdan K, Janius R, Chen G. The effectiveness of combined infrared and hot-air drying strategies for sweet potato. J Food Eng. 2019;241:75–87.
[6] Staniszewska I, Liu Z, Zhou Y, Zielinska D, Xiao H, Pan Z, et al. Microwave-assisted hot air convective drying of whole cranberries subjected to various initial treatments. LWT-Food Sci Technol. 2020;133:109906.
[7] Xu X, Zhang L, Feng Y, Zhou C, Yagoub A, Wahia H, et al. Ultrasound freeze-thawing style pretreatment to improve the efficiency of the vacuum freeze-drying of okra (*Abelmoschus esculentus* (L.) Moench) and the quality characteristics of the dried product. Ultrason Sonochem. 2021;70:105300.
[8] Guo X, Shi L, Xiong S, Hu Y, You J, Huang Q, et al. Gelling properties of vacuum-freeze dried surimi powder as influenced by heating method and microbial transglutaminase. LWT-Food Sci Technol. 2019;99:105–11.
[9] Zhang L, Qiao Y, Wang C, Liao L, Shi D, An K, et al. Influence of high hydrostatic pressure pretreatment on properties of vacuum-freeze dried strawberry slices. Food Chem. 2020;331(12):127203.
[10] Handayani SU, Mujiarto I, Siswanto AP, Ariwibowo D, Atmanto IS, Mustikaningrum M. Drying kinetics of chilli under sun and microwave drying. Mater Today P. 2022;63:153–8.
[11] Shen L, Gao M, Zhu Y, Liu C, Wang L, Kamruzzaman M, et al. Microwave drying of germinated brown rice: Correlation of

drying characteristics with the final quality. Innov Food Sci Emerg. 2021;70:102673.
[12] Li J, Li Z, Li L, Song C, Raghavan GSV, He F. Microwave drying of balsam pear with online aroma detection and control. J Food Eng. 2020;288:110139.
[13] Xiong X, Cao X, Zeng Q, Yang X, Wang Y, Zhang R, et al. Effects of heat pump drying and superfine grinding on the composition of bound phenolics, morphology and microstructure of lychee juice by-products. LWT-Food Sci Technol. 2021;144:111206.
[14] Hou H, Chen Q, Bi J, Wu X, Jin X, Li X, et al. Understanding appearance quality improvement of jujube slices during heat pump drying *via* water state and glass transition. J Food Eng. 2019;272(3):109874.
[15] Ertekin C, Firat MZ. A comprehensive review of thin-layer drying models used in agricultural products. Food Sci Nutr. 2017;57(4):701–17.
[16] Zhou QQ, Ge SF, Ding J, Zhou CL. Study on natural water loss characteristics and mathematical model of CaO conditioned sludge. J Env Eng Technol. 2022;12(3):802–8.
[17] Mbegbu NN, Nwajinka CO, Amaefule DO. Thin layer drying models and characteristics of scent leaves (*Ocimum gratissimum*) and lemon basil leaves (*Ocimum africanum*). Heliyon. 2021;7(1):e05945.
[18] Tunckal C, Doymaz B. Performance analysis and mathematical modelling of banana slices in a heat pump drying system. Renew Energy. 2020;150:918–23.
[19] Peter M, Liu Z, Fang Y, Dou X, Awuah E, Soomro SA, et al. Computational intelligence and mathematical modelling in chanterelle mushrooms' drying process under heat pump dryer. Biosyst Eng. 2021;212:143–59.
[20] Gasa S, Sibanda S, Workneh TS, Laing M, Kassim A. Thin-layer modelling of sweet potato slices drying under naturally-ventilated warm air by solar-venturi dryer. Heliyon. 2022;8:e08949.
[21] Xie Y, Lin Y, Li X, Yang H, Han J, Shang C, et al. Peanut drying: Effects of various drying methods on drying kinetic models, physicochemical properties, germination characteristics, and microstructure. Inform Process Agr; 2022.
[22] Kong D, Wang Y, Li M, Liu X, Huang M, Li X. Analysis of drying kinetics, energy and microstructural properties of turnips using a solar drying system. Sol Energy. 2021;230:721–31.
[23] Dhurve P, Arora VK, Yadav DK, Malakar S. Drying kinetics, mass transfer parameters, and specific energy consumption analysis of watermelon seeds dried using the convective dryer. Mater Today P. 2022;59:926–32.
[24] Biswas R, Afzal M, Hossain MA, Zzaman W. Thin layer modeling of drying kinetics, rehydration kinetics and color changes of osmotic pre-treated pineapple (*Ananas comosus*) slices during drying: Development of a mechanistic model for mass transfer. Innov Food Sci Emerg. 2022;80:103094.
[25] Granella SJ, Bechlin TR, Christ D. Moisture diffusion by the fractional-time model in convective drying with ultrasound-ethanol pretreatment of banana slices. Innov Food Sci Emerg. 2022;76:102933.
[26] Rabha DK, Muthukumar P, Somayaji C. Experimental investigation of thin layer drying kinetics of ghost chilli pepper (Capsicum Chinense Jacq.) dried in a forced convection solar tunnel dryer. Renew Energy. 2017;105:583–9.
[27] Elmizadeh A, Shahedi M, Hamdami N. Comparison of electrohydrodynamic and hot-air drying of the quince slices. Innov Food Sci Emerg. 2017;43:130–5.
[28] Hamdi I, Kooli S, Elkhadraoui A, Azaizia Z, Abdelhamid F, Guizani A. Experimental study and numerical modeling for drying grapes under solar greenhouse. Renew Energy. 2018;127:936–46.
[29] Pratik SG, Sunil CK, Aditi N, Pare A. Effect of microwave assisted hot-air drying temperatures on drying kinetics of dried black gram papad (Indian snack food). Appl Food Res. 2022;11:100144.
[30] Keneni YG, Hvoslef-Eide AT, Marchetti JM. Mathematical modelling of the drying kinetics of *Jatrophacurcas* L. seeds. Ind Crop Prod. 2019;132:12–20.
[31] Halil A. Performance analysis of a solar dryer integrated with the packed bed thermal energy storage (TES) system. Energy. 2019;172(1):1037–52.
[32] Vishnuvardhan RM, Chandramohan VP. Comparison of drying kinetics, thermal and performance parameters during drying guava slices in natural and forced convection indirect solar dryers. Sol Energy. 2022;234(1):319–29.
[33] Huang W, Zhang Y, Qiu H, Huang J, Chen J, Gao L, et al. Drying characteristics of ammonium polyvanadate under microwave heating based on a thin-layer drying kinetics fitting model. J Mater Res Technol. 2022;19:1497–509.
[34] Mbegbu NN, Nwajinka CO, Amaefule DO. Thin layer drying models and characteristics of scent leaves (*Ocimum gratissimum*) and lemon basil leaves (*Ocimum africanum*). Heliyon. 2021;7(1):e05945.
[35] Seerangurayar T, Al-Ismaili AM, Janitha Jeewantha LH, Al-Nabhani A. Experimental investigation of shrinkage and microstructural properties of date fruits at three solar drying methods. Sol Energy. 2019;180:445–55.
[36] Khuthadzo M, Tilahun SW. The kinetics of thin-layer drying and modelling for mango slices and the influence of differing hot-air drying methods on quality. Heliyon. 2021;7(6):e07182.
[37] Onwude D, Hashim N, Janius RB, Nawi NM, Abdan K. Modeling the thin-layer drying of fruits and vegetables: A review. Compr Rev Food Sci F. 2016;15:599–618.
[38] Mohammad G, Mahdi JS, Vahid F, Narges M. Kinetics modelling of color deterioration during thermal processing of tomato paste with the use of response surface methodology. Heat Mass Transf. 2018;54:1–9.
[39] Muñoz-Pina S, Duch-Calabuig A, Ros-Lis José V, Verdejo B, García-España E, Argüelles Á, et al. A tetraazahydroxypyridinone derivative as inhibitor of apple juice enzymatic browning and oxidation. LWT-Food Sci Technol. 2022;154:112778.
[40] Zha Z, Tang R, Wang C, Li Y, Liu S, Wang L, et al. Riboflavin inhibits browning of fresh-cut apples by repressing phenolic metabolism and enhancing antioxidant system. Postharvest Biol Tec. 2022;187:111867.
[41] Muthukumar P, Lakshmi D, Koch P, Gupta M, Srinivasan G. Effect of drying air temperature on the drying characteristics and quality aspects of black ginger. J Stored Prod Res. 2022;97:101966.
[42] Aman K, Palani K, Ivi C, Hangshing L. Analysis of energy consumption, heat and mass transfer, drying kinetics and effective moisture diffusivity during foam-mat drying of mango in a convective hot-air dryer. Biosyst Eng. 2022;219:85–102.

[43] Ramirez C, Astorga V, Nunez H, Jaques A, Simpson R. Anomalous diffusion based on fractional calculus approach applied to drying analysis of apple slices: The effects of relative humidity and temperature. J Food Process Eng. 2017;40(5):e12549.
[44] Selvi KC. Investigating the influence of infrared drying method on linden (*Tilia platyphyllos Scop.*) leaves: Kinetics, color, projected area, modeling, total phenolic, and flavonoid content. Plants. 2020;9(7):916.
[45] Heydari MM, Najib T, Baik O, Tu K, Meda V. Loss factor and moisture diffusivity property estimation of lentil crop during microwave processing. Curr Res Food Sci. 2021;5:73–83.
[46] Pan Y, Guo Y, Huang Q, Zhang W, Zhang Z. Enzymatic browning in relation to permeation of oxygen into the kernel of postharvest areca nut under different storage temperatures. Food Sci Nutr. 2021;9(7):3768–76.
[47] González-Ramírez PJ, Pascual-Mathey LI, García-Rodríguez RV, Jiménez MC, Beristain I, Sanchez-Medina A, et al. Effect of relative humidity on the metabolite profiles, antioxidant activity and sensory acceptance of black garlic processing. Food Biosci. 2022;6:101827.
[48] Sychevskii VA. Calculation of the heat and mass transfer and the strained state of sanitaryware in the process of its convection drying. J Eng Phys Thermophys. 2021;94(3):254–60.
[49] Karaagac O, Kockar H. Optimisation of saturation magnetisation of iron nanoparticles synthesized by hydrogen reduction: Taguchi technique, response surface method, and multiple linear and quadratic regression analyses. J Magn Magn Mater. 2019;473:190–7.